Electronic Supplementary Information for:

Room temperature ferromagnetic manganese boride: low-temperature synthesis of nanoscale α'-MnB

S. Klemenz,[a] M. Fries,[b] M. Dürrschnabel,[c] K. Skokov,[b] H.-J. Kleebe,[c] O. Gutfleisch[b] and B. Albert[a]

[a] *Technische Universität Darmstadt, Eduard-Zintl-Institut of Inorganic and Physical Chemistry, Alarich-Weiss-Str. 12, 64287 Darmstadt, Germany.*

[b] Technische Universität Darmstadt, Institute of Materials Science, Alarich-Weiss-Str. 16, 64287 Darmstadt, Germany

[c] Technische Universität Darmstadt, Institute of Earth Sciences, Schnittspahnstraße 9, 64287 Darmstadt, Germany.

** Correspondence should be addressed to B. Albert.*
Phone: +49 6151 16-22931, E-mail: albert@ac.chemie.tu-darmstadt.de

Table of contents

1. EDX spectrum

EDX spectra were collected using a TEM (description below) with SDD (Fa. Oxford Instruments, Abingdon).

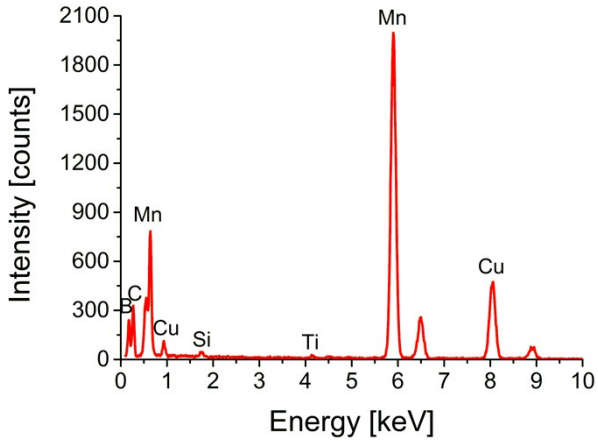

Fig. S1. EDX spectrum after heat treatment (800 °C, 1 h) of α'-MnB nanoparticles.

Table S1. Quantitative EDS analysis of the spectrum shown in **Fig. S1.**

Element	k-factor	wt%	Error wt%	at%
B	7.387	16.98	1.12	50.96
Mn	1.174	83.02	1.12	49.04

2. TEM analysis of untreated precipitate

(High-resolution) Transmission electron microscopy (HRTEM) was performed at a JEOL instrument (2100F, field emission, 200 kV). An air-tight transfer sample-holder was loaded in the glove box.

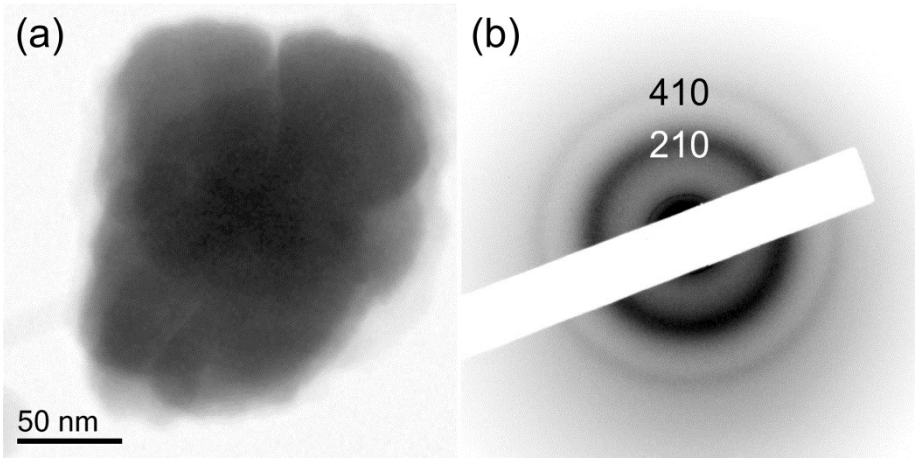

Fig. S2. TEM bright-field image (a) and electron diffraction pattern (b) of MnB nanoparticles without heat treatment.

3. Particle size distribution of untreated precipitate

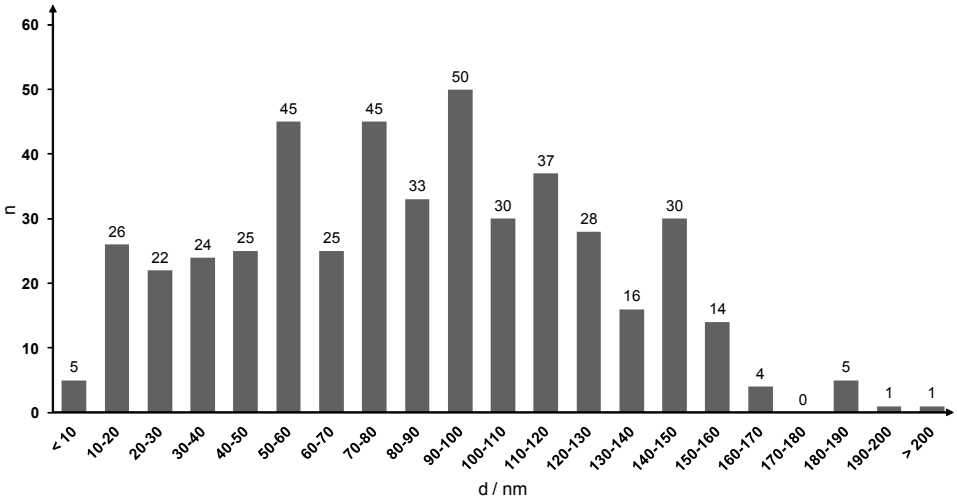

Fig. S3. Size distribution as measured on 466 amorphous MnB nanoparticles using TEM images.

The size distribution for the temperature untreated MnB nanoparticles (Figure S3) was derived from measuring 466 different particles as seen in TEM images comparable to Figure S2. The distribution for crystallized MnB particles was derived from measuring 54 different particles (Figure S4). Due to the broad distribution of sizes and the low number of particles a mean diameter for the crystallized samples is not representative.

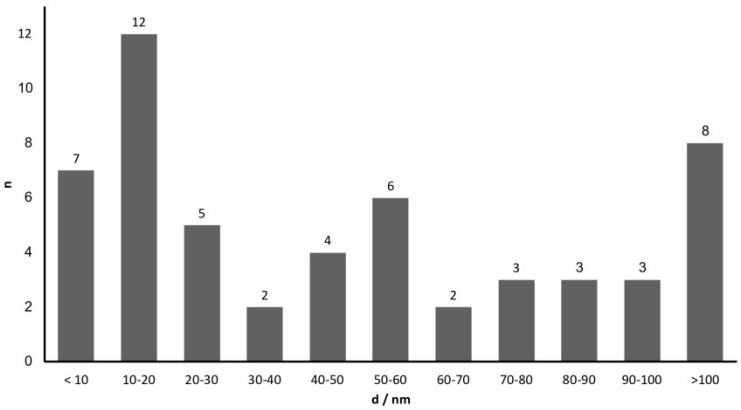

Firg. S4. Size distribution as measured on 54 amorphous MnB nanoparticles using TEM images.

4. TGA/DSC and ex-situ XRD

Thermogravimetric analysis and differential scanning calorimetry (TGA/DSC) were performed using a simultaneous thermal analyzer (STA 449 F3 Jupiter, Netzsch, Selb) in a BN crucible from room temperature till 1673 K with steps of 20 K/min (**Fig. S4.**).

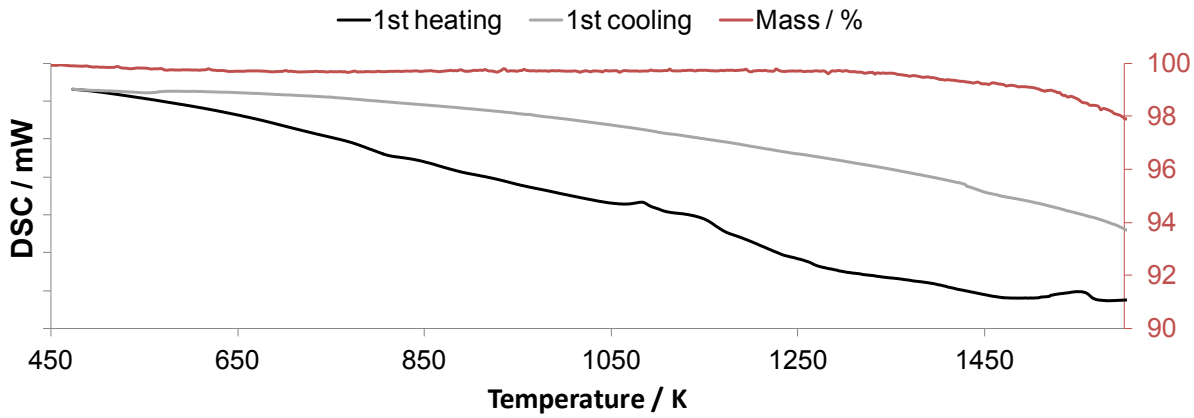

Fig. S5. TGA/DSC curve of a pre-heated sample (1073 K, 2 h) measured till 1673 K.

For X-ray powder diffraction (XRD) the samples were sealed under argon into glass capillaries and measured on a powder diffractometer (Stadi-P, Fa. Stoe, Darmstadt) using Mo-$K_{\alpha 1}$ radiation. Measurements were performed *ex-situ* on samples after heating to 873, 1073, 1323, 1573, and 1673 K (**Fig. S5.**).

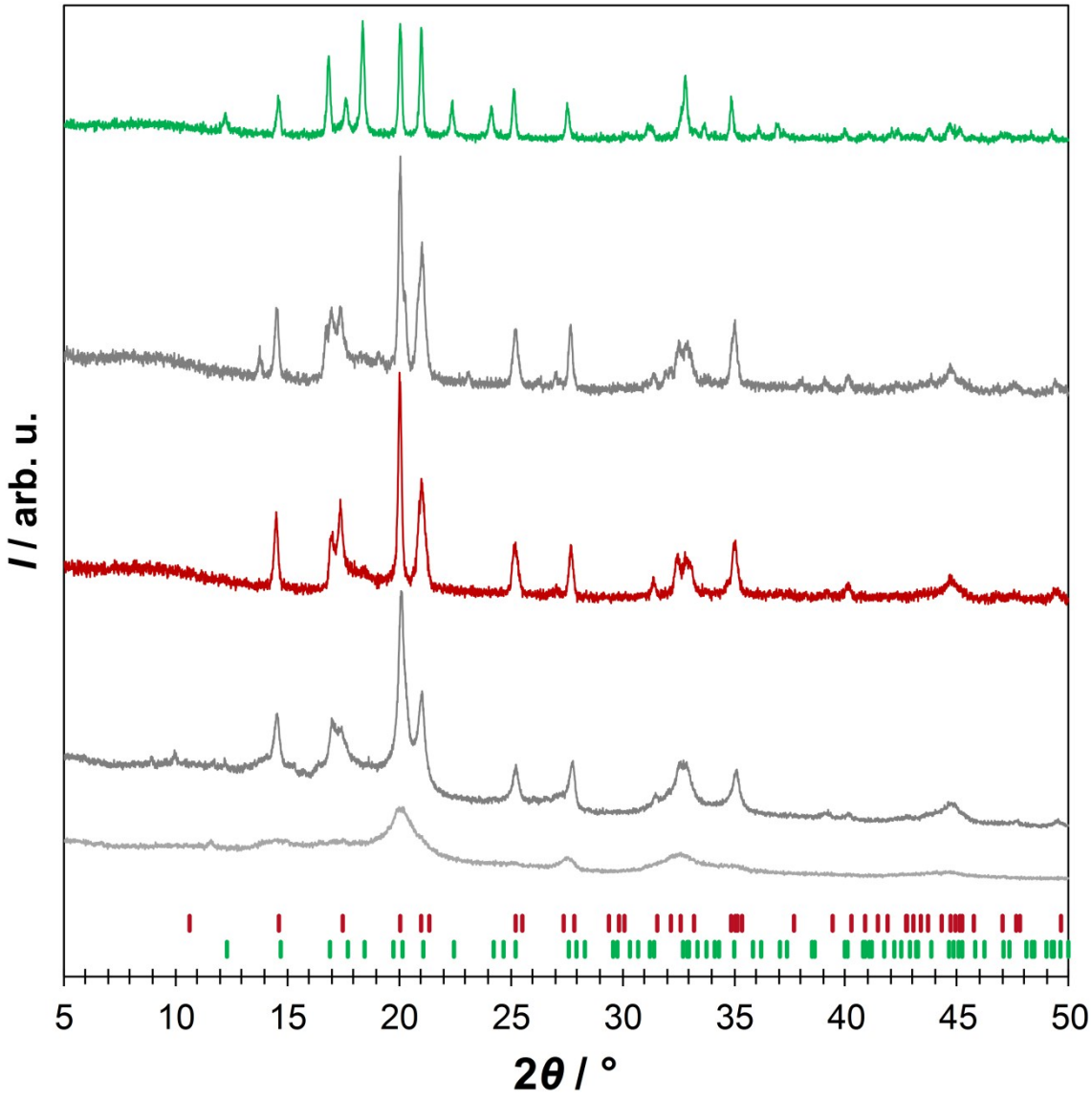

Fig S6. Diffraction patterns of MnB nanoparticles after heating to 873 (light gray), 1073 (gray), 1323 (red), 1573 (dark gray), and 1673 K (green). Reflex positions are given for β-MnB[1] (green) and α-MnB[2] (red).

5. DIFFaX structure analysis

The DIFFaX simulation shown in the paper was done using the parameters shown in Table S2 and the layer transition probabilities in Table S3 (for layer definition see Fig. S8).

Table S2. DIFFaX simulation data.

function types:	background function: gaussian profile function: pseudo-Voigt			
Λ	0.7093 Å			
layer width:	infinite layer with (*a*'*b*')			
number of layers:	infinite stacking along *c*'			
ensemble:	Recursive			
symmetrie:	no given symmetry determined point group: 2/m determination limit: < 1 ppm			
lattice parameters:	*a*' = 295.43 pm	*b*' = 412.63 pm	*c*' = 559.88 pm	α = β = γ = 90 °

layer A	***x/a***	***y/b***	***z/c***	**B**	**Occupation**
Mn1	0.75	0.17688	0.1198	0.03	1
Mn2	0.25	0.6198	0.32312	0.03	1
Mn3	0.75	0.42688	0.6198	0.03	1
Mn4	0.25	0.8698	0.82312	0.03	1
B1	0.75	0.865	0.5332	0.03	1
B2	0.25	0.365	0.9668	0.03	1
B3	0.75	0.615	0.0332	0.03	1
B4	0.25	0.115	0.4668	0.03	1
layer B	***x/a***	***y/b***	***z/c***	**B**	**Occupation**
Mn1	0.75	0.17688	0.1198	0.03	1
Mn2	0.25	0.6198	0.32312	0.03	1
Mn3	0.75	0.92688	0.6198	0.03	1
Mn4	0.25	0.3698	0.82312	0.03	1
B1	0.75	0.615	0.0332	0.03	1
B2	0.25	0.115	0.4668	0.03	1
B3	0.75	0.365	0.5332	0.03	1
B4	0.25	0.865	0.9668	0.03	1
layer C	***x/a***	***y/b***	***z/c***	**B**	**Occupation**
Mn1	0.75	0.67688	0.1198	0.03	1
Mn2	0.25	0.1198	0.32312	0.03	1
Mn3	0.75	0.42688	0.6198	0.03	1
Mn4	0.25	0.8698	0.82312	0.03	1
B1	0.75	0.115	0.0332	0.03	1
B2	0.25	0.615	0.4668	0.03	1
B3	0.75	0.865	0.5332	0.03	1
B4	0.25	0.365	0.9668	0.03	1
layer D	***x/a***	***y/b***	***z/c***	**B**	**Occupation**
Mn1	0.75	0.67688	0.1198	0.03	1
Mn2	0.25	0.1198	0.32312	0.03	1
Mn3	0.75	0.92688	0.6198	0.03	1
Mn4	0.25	0.3698	0.82312	0.03	1
B1	0.75	0.115	0.0332	0.03	1
B2	0.25	0.615	0.4668	0.03	1
B3	0.75	0.365	0.5332	0.03	1
B4	0.25	0.865	0.9668	0.03	1

Table S3. Transition probabilities of layer A, B, C, D to follow layer A, B, C, D.

		following layer			
		A	**B**	**C**	**D**
starting layer	**A**	0.4	0.2	0.1	0.3
	B	0.15	0.05	0.8	0.0
	C	0.1	0.75	0.1	0.05
	D	0.8	0.0	0.1	0.1

6. Mn-Mn distances in MnB modifications

Mn-Mn distances for MnB in α- and β-modification. In MnB the coordination sphere of Mn can be described as distorted trigonal prism with average Mn-Mn distance d_1 of 266.0 pm or 267.9 pm and distorted planar square with average Mn-Mn distance d_2 of 297.9 pm or 297.2 pm for α- and β-modification respectively (Fig. S6). The coordination spheres are distorted, thus the average Mn-Mn distances d_1 and d_2 have can be split. The actual Mn-Mn distances in the trigonal prism are $d_{1,1}$ and $d_{1,2}$ and in the planar square $d_{2,1}$ and $d_{2,2}$ (Table S4).

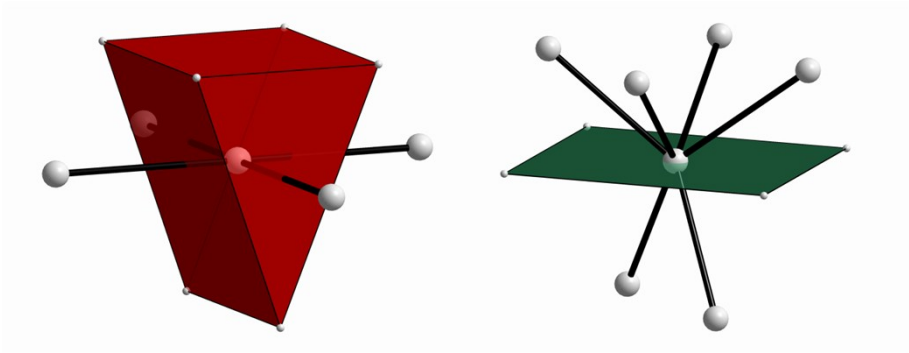

Fig. S7. Coordination sphere for Mn (white balls) in MnB (distorted trigonal prism (red) and distorted square (green)).

Table S4. Mn-Mn distances in α- and β-MnB[1].

Mn-Mn	# of Mn	α-MnB	β-MnB	Mn-Mn	# of Mn	α'-MnB	β-MnB
d_1	6	*266.0 pm*	*267.9 pm*	$d_{1,1}$	4	265.4 pm	266.8 pm
				$d_{1,2}$	2	267.4 pm	270.1 pm
d_2	4	*297.9 pm*	*297.2 pm*	$d_{2,1}$	2	295.3 pm	296.7 pm
				$d_{2,2}$	2	300.5 pm	297.7 pm

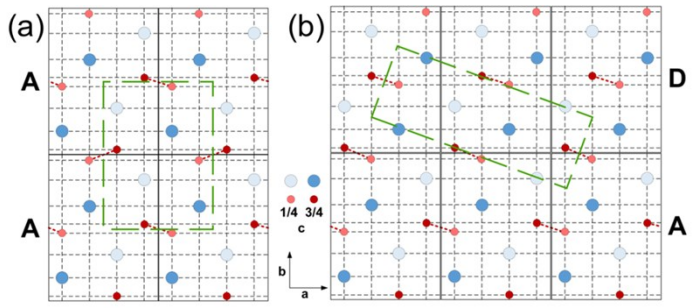

Fig. S8. Layers defined to refine the structure types FeB (a) and CrB (b) with the unit cell drawn in green.

7. References

[1] R. Kiessling, *Acta Chem Scand* **1950**, 146–159.